Annals of Nuclear Medicine Vol. 15, No. 1, 21–26, 2001

Diagnostic accuracy of simultaneous acquisition of transmission and emission data with technetium-99m transmission source on thallium-201 myocardial SPECT

Yoichi OHYAMA,* Seiji TOMIGUCHI,* Tomohiro KIRA,* Mitsuko KIRA,* Akinori TSUJI,* Akihiro KOJIMA,* Masanori MATSUMOTO,** Mutsumasa TAKAHASHI,* Yoshito INOBE*** and Hirofumi YASUE***

*Department of Radiology and ***Department of Cardiology, Kumamoto University School of Medicine
**Department of Radiological Technology, Kumamoto University College of Medical Science

Purpose: This study evaluates not only the clinical usefulness but also the problems in attenuation correction for thallium-201 (Tl-201) myocardial SPECT by means of simultaneous transmission and emission data acquisition in the detection of coronary artery disease (CAD).
Methods: A three-detector SPECT system equipped with a Tc-99m line source and fan-beam collimators was used for simultaneous transmission and emission data acquisition for Tl-201 myocardial SPECT in 73 patients (18 patients for normal database and 55 patients for the evaluation of diagnostic accuracy). Attenuation-corrected (AC) images and non-attenuation-corrected (NC) images were reconstructed with an iterative maximum-likelihood estimation-corrected (ML-EM) algorithm. Both sets of images were reoriented into the short axis. Normal database polar maps were constructed from the AC and NC images for quantitative analysis.
Results: There was a significant difference in specificity between NC and AC images in the RCA territory and those in specificity and accuracy in the LCX territory. There was no significant difference in sensitivity found between NC and AC images in either territory, but sensitivity in both territories tended to decrease with attenuation correction. In the LAD territory, there were various changes in sensitivity and specificity observed with attenuation correction in cases with each quantitative criterion.
Conclusions: Diagnostic performance of significant stenosis in the RCA and LCX territories quantitatively improved with attenuation correction because of an increase in specificity, but no significant improvement in diagnostic performance was obtained in the LAD territory with attenuation correction. We recommend combined interpretation of AC and NC images and careful evaluation of any SPECT image by means of transmission computed tomography.

Key words: transmission computed tomography, attenuation correction, Thallium-201 myocardial SPECT, coronary artery disease

INTRODUCTION

THALLIUM-201 (Tl-201) single-photon emission computed tomography (SPECT) has become a well established imaging method for evaluating the presence and extent of coronary artery disease (CAD). SPECT provides higher contrast images and improves overall detection of CAD,[1,2] but attenuation by the breast and diaphragm causes a certain loss of specificity in the detection of CAD. The most promising method for correcting Tl-201 SPECT images for attenuation is to measure attenuation distribution by means of transmission computed tomography (TCT).[3–8]

Tung et al.[5] used a three-detector SPECT system with a collimated technetium-99m (Tc-99m)-line source opposite a detector fitted with a 65-cm fanbeam collimator

Received October 28, 2000, revision accepted November 13, 2000.

For reprint contact: Yoichi Ohyama, M.D., Department of Radiology, Kumamoto University School of Medicine, 1–1–1 Honjo, Kumamoto 860–8556, JAPAN.

to perform simultaneous transmission and emission data acquisition for Tl-201 myocardial SPECT. With this system, attenuation correction increased relative intensity in the inferior wall and posterior septal wall of the left ventricle. Preliminary results of patient studies showed that attenuation correction might improve sensitivity and specificity in the evaluation of CADs, but clinical validation might be necessary for their studies to define the diagnostic benefits.

The purpose of this study was to assess the diagnostic performance of attenuation-corrected (AC) stress Tl-201 myocardial SPECT for the identification of CAD.

MATERIALS AND METHODS

Patients

Simultaneous acquisition of transmission and emission computed tomographic (ECT) data was performed on 73 patients who were referred for stress myocardial perfusion imaging. They consisted of 18 patients (9 men and 9 women; mean age, 64.8 ± 7.0 years) for sex-specific normal database and 55 patients (39 men and 16 women; mean age, 62.6 ± 15.3 years) for the evaluation of diagnostic performance of stress Tl-201 myocardial SPECT. They were all suspected of CAD and underwent a coronary angiography. All 18 patients for the normal database had no significant stenosis in the coronary artery on coronary angiography (CAG). There were 7 patients without CAD and 48 cases with CAD (15 with myocardial infarction, 33 with angina pectoris) classified by the presence of over 75% stenosis of luminal diameter on coronary angiography. Informed consent was obtained from all patients. Of 48 patients with CAD, 26 cases had an organic stenosis in the left anterior descending artery (LAD), 12 in the right coronary artery (RCA) and 12 in the left circumflex artery (LCX).

No patient was excluded because of coexisting hypertension, valvular heart disease or cardiomyopathy.

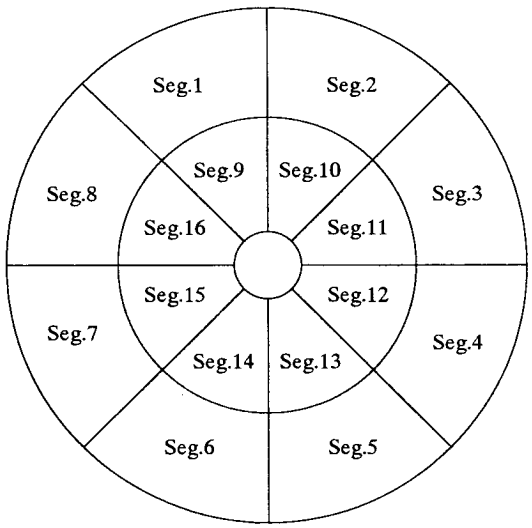

Fig. 1 Schematic display of each segment. A polar map was divided into 16 segments, corresponding to the vascular territories. LAD territory includes seg 1–2, seg 7–10 and seg 15–16. RCA territory includes seg 5–6 and seg 13–14. LCX territory includes seg 3–4 and seg 11–12.

Data Acquisition and Processing of TCT/ECT Data

A PRISM 3000 SPECT System (Ohio Imaging of Picker International, Bedford Heights, Ohio) was used to perform simultaneous transmission and emission data acquisition. All three detectors were equipped with low energy, high resolution fanbeam collimators with a focal length of 65 cm. The source holder was positioned opposite and parallel to one of the three detectors fitted with a fanbeam collimator. The source was collimated so that an aperture of approximately 40 degrees was obtained along the line source, which was 50.8 cm in length and 1.2 mm in diameter. The transmission source was Tc-99m and the emission source was Tl-201 for patient studies.

The line source was filled with 740 MBq of Tc-99m. Transmission and emission data were collected with the fanbeam collimators. All three detectors acquired the data in two energy windows. One 15% window was centered at about 140 keV for transmission data and one 30% window was centered at about 73 keV for the emission data. Projections were digitized onto a 64 × 64 matrix. A total of 60 projections were sampled over 360 degrees for each detector by using a body contoured orbit. Each view

Table 1 Diagnostic performance of AC and NC Tl-201 myocardial SPECT in LAD

No. of segments	SD						2SD						2.5SD					
	Sensitivity (%)		Specificity (%)		Accuracy (%)		Sensitivity (%)		Specificity (%)		Accuracy (%)		Sensitivity (%)		Specificity (%)		Accuracy (%)	
	AC	NC	AC	NC	AC	NC	AC	NC	AC	NC	AC	NC	AC	NC	AC	NC	AC	NC
1	88.5	92.3	41.4	41.4	60.0	65.5	84.6	84.6	65.5	72.4	74.5	78.2	76.9	84.6	72.4	79.3	74.5	81.8
2	73.1	76.9	55.2	58.6	63.6	67.3	73.1	69.2	69.0	79.3	71.0	74.5	69.2	69.2	82.8	82.8	76.4	76.4
3	73.1	69.2	58.6	65.5	65.5	67.3	65.4	65.4	86.2	82.8	76.4	74.5	65.4	65.4	89.7	86.2	78.2	76.4
4	65.4	69.2	75.9	72.4	70.9	70.9	61.5	50.0	86.2	82.8	74.6	67.3	57.7	46.2	96.6	86.2	78.2	67.3

*: significant difference ($p < 0.05$) AC: attenuation-corrected, NC: non-attenuation-corrected

No. of segments: Number of abnormal segments in each territory. (1; more than 1 segment, 2; more than 2 segments, 3; more than 3 segments, 4; more than 4 segments)

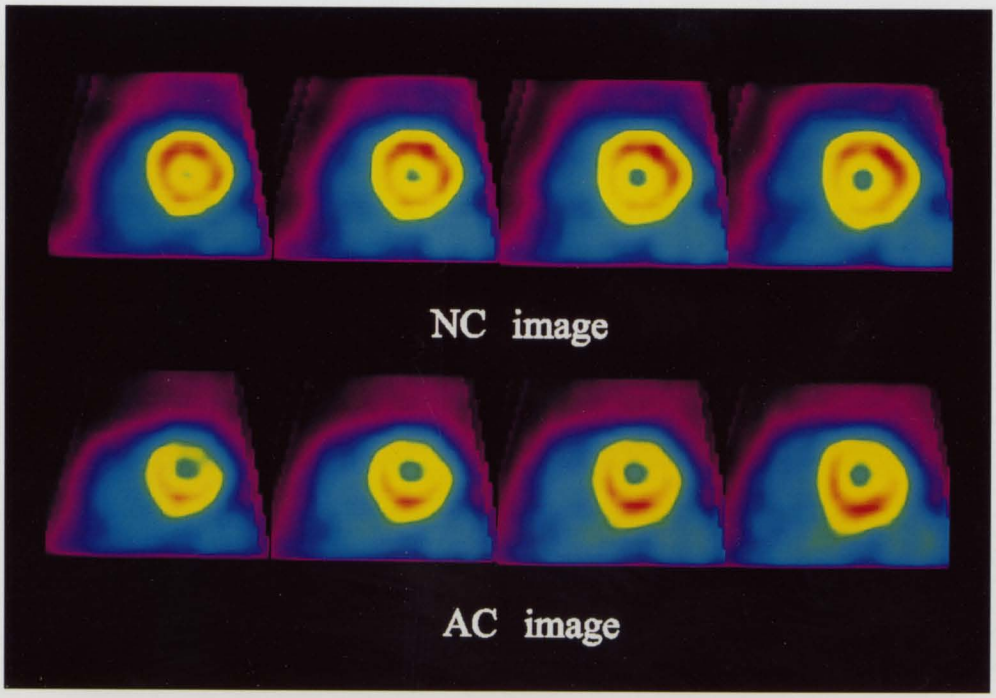

Fig. 2 AC images and NC images. Short axial images of a 54-year-old male with normal coronary artery. In NC images, LAD territory shows normal perfusion. However in AC images, LAD territory shows hypoperfusion.

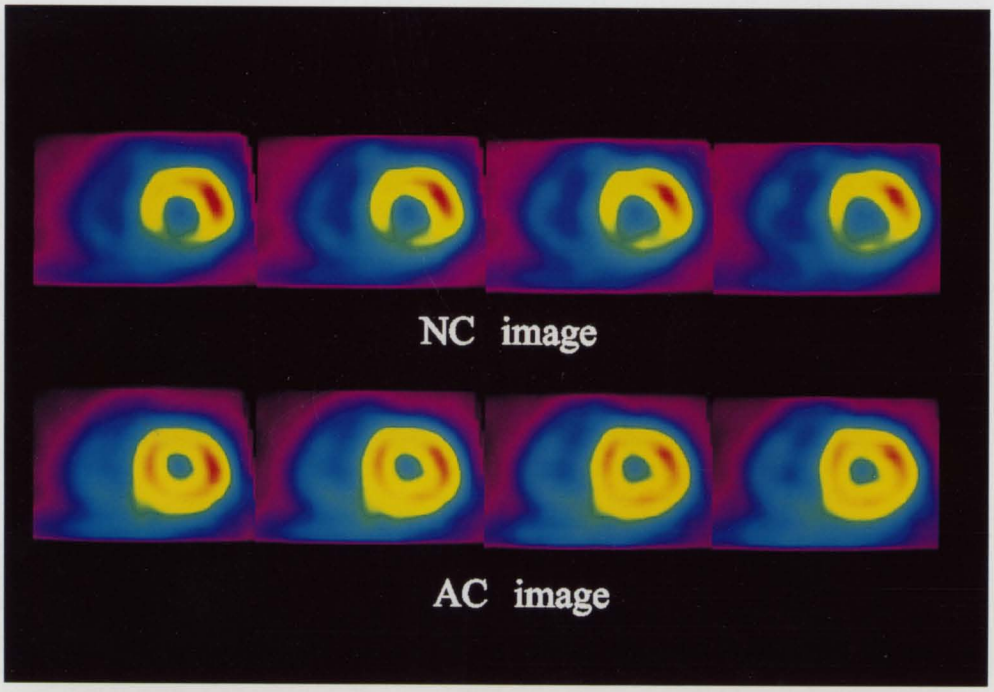

Fig. 3 AC images and NC images. Short axial images of a 63-year-old female with normal coronary artery. In NC images, RCA territory shows hypoperfusion. However in AC images, RCA territory shows normal perfusion.

was acquired for 10 seconds.

After removal of cross-talk contamination from the transmission and emission data, the transmission data were converted to projections of linear attenuation coefficients by taking the natural logarithm of the ratio of the incident flux to the measured transmission counts. These

Table 2 Diagnostic performance of AC and NC Tl-201 myocardial SPECT in RCA

No. of segments	SD						2SD						2.5SD					
	Sensitivity (%)		Specificity (%)		Accuracy (%)		Sensitivity (%)		Specificity (%)		Accuracy (%)		Sensitivity (%)		Specificity (%)		Accuracy (%)	
	AC	NC	AC	NC	AC	NC	AC	NC	AC	NC	AC	NC	AC	NC	AC	NC	AC	NC
1	75.0	91.7	44.2	25.6	50.9	40.0	66.7	83.3	69.8	48.8	69.1	56.4	66.7	83.3	76.7*	51.2	74.5	58.2
2	58.3	91.7	69.8	51.2	67.3	60.0	50.0	75.0	83.7	72.1	76.4	72.2	41.7	66.7	90.7	81.4	80.0	78.2

*: significant difference ($p < 0.05$) AC: attenuation-corrected, NC: non-attenuation-corrected
No. of segments: Number of abnormal segments in each territory. (1; more than 1 segment, 2; more than 2 segments)

Table 3 Diagnostic performance of AC and NC Tl-201 myocardial SPECT in LCX

No. of segments	SD						2SD						2.5SD					
	Sensitivity (%)		Specificity (%)		Accuracy (%)		Sensitivity (%)		Specificity (%)		Accuracy (%)		Sensitivity (%)		Specificity (%)		Accuracy (%)	
	AC	NC	AC	NC	AC	NC	AC	NC	AC	NC	AC	NC	AC	NC	AC	NC	AC	NC
1	90.9	100.0	38.6*	18.2	49.1	34.5	72.7	81.8	70.5*	38.6	70.9*	47.3	72.7	81.8	75.0*	45.5	74.5*	52.7
2	81.8	90.9	61.4*	34.1	65.5*	45.5	72.7	81.8	79.5	63.6	78.2	67.3	63.6	72.7	86.4	72.7	81.8	72.7

*: significant difference ($p < 0.05$) AC: attenuation-corrected, NC: non-attenuation-corrected
No. of segments: Number of abnormal segments in each territory. (1; more than 1 segment, 2; more than 2 segments)

projections were reconstructed with 20 iterations of the iterative maximum-likelihood estimation-maximization (ML-EM) algorithm. Reconstructed attenuation coefficients for the 140 keV Tc-99m were then transformed to the coefficients for the 73 keV energy of Tl-201. The conversion was based on the assumption that the coefficient changed linearly between 140 keV and 73 keV.

The cross-talk corrected emission projection data were reconstructed with 20 iterations of the iterative ML-EM algorithm. Attenuation factors were calculated as exponentials of the partial line integrals for the attenuation distribution from the pixel of interest to the detector. These factors were retrieved from on-board memory during the projection and backprojection operations. The reconstructed AC images were filtered with a three-dimensional low-pass filter to reduce image noise. Transaxial images were reformatted to produce short axis, vertical long axis, and horizontal long axis displays. For comparison, non-attenuation-corrected (NC) images were also reconstructed with 20 iterations of the iterative ML-EM algorithm.

Data Analysis

Quantitative results were generated from the tracer distributions in a polar map format compared with a database of normal distributions. The distal-to-basal rings of the polar maps were constructed from maximum-count circumferential profiles of short-axis slices. The polar maps were normalized to the maximum count within each map. To account for differences in the photon attenuation patterns of male and female patients, gender-specific databases were constructed for the quantitative analysis. A polar map was divided into 16 segments. Segments and the vascular territories used to determine the localization of the perfusion defects in these maps are shown in Figure 1.

They consisted of 8 segments (seg 1–2, seg 7–10 and seg 15–16) of the LAD territory, 4 (seg 5–6 and seg 13–14) of RCA territory and 4 (seg 3–4 and seg 11–12) of the LCX territory (Fig. 1). The mean pixel counts in each segment more than standard deviation (SD), 2SD, and 2.5 SD respectively, below the normal mean of the appropriate database values were regarded as abnormal. Abnormal thresholds in each territory were assessed by comparison with the number of abnormal segments in each territory. In the LAD territory, from 1 to 4 abnormal segments were selected, and 1 or 2 segments in RCA and LCX territories for the analysis of both the AC and NC maps. The McNemar's test was used to determine differences in paired data samples. Statistical significance was defined as $p < 0.05$.

RESULTS

The diagnostic performance for the detection of a coronary arterial stenosis was evaluated in each territory, and in 55 patients. Sensitivity, specificity and accuracy for the localization of a disease in each of the three main coronary distributions are shown in Tables 1 to 3.

In the LAD territory, there was a tendency to an increase in specificity when considering a greater number of abnormal segments as positive or a higher threshold level as positive (Table 1). There were various changes in sensitivity observed between AC and NC images, but no significant difference was observed between AC and NC images in diagnostic performance. An increase in counts in the inferior wall and a relative reduction in tracer distribution in the anterior wall appeared with attenuation

correction in some cases (Fig. 2). This phenomenon may result in the various changes in sensitivity and specificity in the LAD territory with attenuation correction.

In the RCA and LCX territories, improvement in radioactivity in the inferior wall was obtained with attenuation correction in the normal cases as shown in Figure 3. Diagnostic accuracy improved on AC images as compared with NC images because of an increase in specificity of all criteria (Tables 2 and 3). In the RCA territory, there was a significant difference between NC and AC images in specificity. And in the LCX territory, there were significant differences between NC and AC images in specificity and accuracy. Although sensitivity decreased with attenuation correction in both territories, there was no significant difference between NC and AC images in sensitivity (Tables 2 and 3).

DISCUSSION

The clinical validation of attenuation correction with a three detector camera has been shown in Tc-99m sestamibi myocardial perfusion imaging.[9] Ficaro et al.[9] published the validation of a system with a fanbeam collimator for the transmission data obtained from an Am-241 line source. The other two detectors collecting the emission data of Tc-99m sestamibi were equipped with parallel hole collimators, in order to reduce truncation. For the detection of CAD, the quantitative results demonstrated that the AC images more clearly differentiated stenosed from nonstenosed vessels compared with the NC images and that the improvement in diagnostic accuracy resulted primarily from increased sensitivity. They remarked that the increased sensitivity can be attributed to the uniformity of the mean and variance distributions of the AC polar maps compared with the normal NC maps. The uniform distribution of the AC polar maps provides stricter thresholds for the detection of CAD, resulting in improved sensitivity without loss of specificity.

In this study, the increase in accuracy for disease localization by means of the AC images resulted from an increase in specificity in the RCA and LCX territories, but no changes in specificity in the LAD territory were observed on the AC polar maps compared with the NC polar maps. Recently, Vidal et al.[10] reported that an increase in specificity was obtained with attenuation correction in the RCA territory, but the sensitivity of defect detection was significantly reduced in the LAD territory by visual analysis. In our results, quantitative evaluation also shows an improvement in diagnostic performance in the RCA and LCX territories. No improvement in diagnostic performance was obtained in the LAD territory with attenuation correction.

Ficaro et al.[9] reported that the apex in the AC images showed a significant decrease in activity relative to the base, which appeared consistent with anatomic wall thinning, but they did not emphasize the significant decrease in activity in the anteroapical wall on the AC images. On the other hand, Miron et al.[11] used a triple head camera equipped with a Tc-99m line source for Tl-201 myocardial SPECT imaging, which was the same system as we used in the present study. A preliminary study of 29 stress images revealed that there was overcorrection of the inferior wall, most likely due to increased scatter from the liver accumulation. Overcorrection of the inferior wall resulted in a relative decrease in tracer distribution in the LAD territory. A decrease in specificity in the LAD territory was observed in some criteria and it was caused by the overcorrection of the inferior wall with attenuation correction. The decrease in sensitivity in the RCA and LCX territories was also caused by overcorrection of the inferior wall. Reconstructed counts are artificially enhanced in the regions of high tissue density when scattered events are not removed from the projections prior to attenuation correction.[12–14] This is one of the main reasons why a decrease in activity appears in the anterior wall with attenuation correction.[15] Case et al.[16] developed a clinical protocol for performing both attenuation and scatter correction for Tl-201 myocardial SPECT studies with a triple head camera. Their results revealed that though attenuation and scatter diminished in the images, the reconstructions still possess residual non-uniformities due to poor sampling, partial volume effects, and cardiac motion. To obtain true Tl-201 myocardial SPECT images, further development of the hardware and software of the gamma camera systems is necessary.

In conclusion, by attenuation correction with a triple head gamma camera equipped with fanbeam collimators and with a Tc-99m line source for transmission, the diagnostic accuracy of the localization of a disease was improved on AC images compared with NC images, evidenced by an increase in specificity in the RCA and LCX territories. Nevertheless, change in sensitivity and specificity in the LAD territory were observed because an increase in counts in the inferior wall and a relative reduction in tracer distribution in the anterior wall appeared with attenuation correction. Diagnosis of significant stenosis in the RCA and LCX territories quantitatively improved with attenuation correction because of an increase in specificity, but no significant improvement in diagnostic performance was obtained in the LAD territory with attenuation correction. We recommend combined interpretation of AC and NC images and careful evaluation of any simultaneous emission/transmission imaging protocol in patients before using such a protocol.

REFERENCES

1. DePasquale E, Nody C, DePuey G, Garcia E, Pilcher G, Bredlau C, et al. Quantitative rotational thallium-201 tomography for identifying and localizing coronary artery disease. *Circulation* 1988; 77: 316–327.
2. Mahmarian JJ, Boyce TM, Goldberg RK, Cocanougher

MK, Roberts BR, Verani MS. Quantitative exercise thallium-201 single-photon emission computed tomography for the enhanced diagnosis of ischemic heart disease. *J Am Coll Cardiol* 1990; 15: 318–329.
3. Tsui BMW, Gullberg GT, Edgerton ER, Ballard JG, Perry JR, McCartney WH, et al. Correction of nonuniform attenuation in cardiac SPECT imaging. *J Nucl Med* 1989; 30: 497–507.
4. Frey EC, Tsui BMW, Perry JR. Simultaneous acquisition of emission and transmission data for improved Thallium-201 cardiac SPECT imaging using a Technetium-99m transmission source. *J Nucl Med* 1992; 33: 2238–2245.
5. Tung CH, Gullberg GT, Zeng GL, Christian PE, Datz FL, Morgan HT. Non-uniform attenuation correction using simultaneous transmission and emission converging tomography. *IEEE Trans Nucl Sci* 1992; 39: 1134–1143.
6. Jaszczak RJ, Gilland DR, Hanson MW, Jang S, Greer KL, Coleman RE. Fast transmission CT for determining attenuation maps using a collimated line source, rotatable air-copper-lead attenuators and fan-beam collimation. *J Nucl Med* 1993; 34: 1577–1586.
7. Ficaro EP, Fessler JA, Rogers WL, Schwaiger M. Comparison of Americium-241 and Technetium-99m as transmission sources for attenuation correction of thallium-201 SPECT imaging of the heart. *J Nucl Med* 1994; 35: 652–663.
8. Ficaro EP, Fessler JA, Ackermann RJ, Rogers WL, Corbett JR, Schwaiger M. Simultaneous transmission-emission Thallium-201 cardiac SPECT: effect of attenuation correction on myocardial tracer distribution. *J Nucl Med* 1995; 36: 921–931.
9. Ficaro EP, Fessler JA, Shreve PD, Kritzman JN, Rose PA, Corbett JR. Simultaneous transmission/emission myocardial perfusion tomography: diagnostic accuracy of attenuation corrected Tc-99m sestamibi single-photon emission computed tomography. *Circulation* 1996; 93: 463–473.
10. Vidal R, Buvat I, Darcourt J, Migneco O, Desvignes P, Baudouy M, et al. Impact of attenuation correction by simultaneous emission/transmission tomography on visual assessment of Tl-201 myocardial perfusion images. *J Nucl Med* 1999; 40: 1301–1309.
11. Miron SD, Conant RG, Sodee DB, Amini SB. Clinical evaluation of simultaneous transmission-emission SPECT myocardial perfusion images (STEP). [Abstract] *J Nucl Med* 1995; 36: 12P.
12. Meikle SR, Hutton BF, Bailey DL. A transmission-dependent method for scatter correction in SPECT. *J Nucl Med* 1994; 35: 360–367.
13. King MA, Xia W, DeVries DJ, Pan TS, Villegas BJ, Dahlberg S, et al. A Monte Carlo investigation of artifacts caused by liver uptake in single-photon emission computed tomography perfusion imaging with technetium 99m-labeled agents. *J Nucl Cardiol* 1996; 3 (1): 18–29.
14. Prvulovich EM, Lonn AHR, Bomanji JB, Jarritt PH, Ell PJ. Effect of attenuation correction on myocardial thallium-201 distribution in patients with a low likelihood of coronary artery disease. *Eur J Nucl Med* 1997; 24: 266–275.
15. Maniawski PJ, Miller SD, Morgan HT. Combined attenuation and scatter correction significantly reduces the effect of extra-cardiac activity on Tl-201 myocardial perfusion SPECT. [Abstract] *J Nucl Med* 1996; 37: 214P.
16. Case JA, King MA, Dalhberg ST. Results of attenuation and scatter correction in clinical cardiac Tl-201 SPECT perfusion imaging. [Abstract] *J Nucl Med* 1996; 37: 212P.